行政院國家科學委員會專題研究計畫　成果報告

風扇流中渦流產生器對流場結構及熱傳增益影響之探討

計畫類別：個別型計畫
計畫編號：NSC91-2212-E-032-007-
執行期間：91 年 08 月 01 日至 92 年 07 月 31 日
執行單位：淡江大學航空太空工程學系(所)

計畫主持人：陳增源

報告類型：精簡報告

處理方式：本計畫可公開查詢

中　華　民　國 92 年 10 月 23 日

本計畫研究成果將刊登期刊 “Experimental Thermal and Fluid Science”,

現正付印中, 並已於 8/27/2003 線上刊登(available on line)

Flow Structures and Heat Transfer Characteristics in Fan Flows with and without Delta-wing Vortex Generators

T. Y. Chen and H. T. Shu

Department of Aerospace Engineering

Tamkang University, Taiwan, R. O. C.

Abstract

Effects of an external delta-wing vortex generator on the flow and heat transfer characteristics in fan flows and uniform flows were experimentally investigated and compared. A heated plate, installed on the bottom wall of a duct, was used as the heat transfer surface. Three-component mean and fluctuating velocity measurements were conducted using a laser Doppler velocimetry to characterize the flow structures and to obtain the near-wall flow parameters, including the axial mean velocity, axial vorticity and turbulent kinetic energy. Temperatures on the heat transfer surface were measured using thermocouples to obtain the Nusselt numbers. Results show that the external delta-wing vortex generator in fan flows has little overall effect on the near-wall averaged axial mean velocity and axial vorticity, but increases the turbulent kinetic energy, in the investigated *X/D* ranges. The increase in the turbulent kinetic energy by the delta-wing has little effect on heat transfer in the inherently vortical fan flows. Consequently, the delta-wing vortex generator in fan flows has little effect on the heat transfer augmentation.

Keywords: fan flow, vortex generator, heat transfer

1. Introduction

Extensive studies have been conducted on the heat transfer enhancement using turbulators in simulated heat exchangers, turbine blades and so on [1-14]. The turbulator usually generates high turbulence vortical motion in uniform flows, which may change the mean velocity fields, modify the flow turbulence properties and the structures of the near wall layers in the velocity boundary layer. These, in turn, cause modifications in the heat transfer characteristics. Edwards and Alker [1] investigated convective heat transfer augmentation using three-dimensional surface protrusions in the form of cubes and vortex generators. The cube was found to produce the highest local improvement, but the vortex generator effect extended further downstream. Russell et al. [2] studied the heat transfer enhancement on plate fin surfaces on which local vortex generators produced a set of contra-rotating vortices. Their study showed that considerable heat transfer enhancement occurred, and the pressure loss penalty associated with vortex generators was modest. Eibeck and Eaton [3] experimentally examined the heat transfer effects of an isolated longitudinal vortex embedded in a turbulent boundary layer. They found that the longitudinal vortex effects on the Stanton number were attributed largely to the distortion in the mean velocity field. Fiebig and his group [5-8] conducted systematic experimental investigations on heat transfer

enhancement and induced drag using delta wings, rectangular wings, delta winglets and rectangular winglets in channel uniform flows. They found that the heat transfer was increased up to 60-degree angle of attack. The heat transfer enhancement per unit vortex generator area was the highest for delta wings followed by delta winglets and rectangular winglets [5]. However, the results from Ref. 7 showed that delta winglets produced better heat transfer performance than wings. No explanations were given on these contradictory results. Their studies also showed that the vortices in the wake of the second row were more unsteadiness than the first-row vortices [6]. A pair of delta winglets performed slightly better than a pair of rectangular winglets at higher angles of attack and Reynolds numbers [8]. The results from studies by Biswas et al. [9,10] indicated that the flow loss due to the winglet-pair was less than that due to the wing, and the zone of poor heat transfer as it was observed with the wing could be avoided by using winglet-pair. The use of winglet-pair appeared to be a more attractive augmentation technique. Hwang et al. [12] and Liou et al. [13] investigated the effects of ridge shapes and rib-arrays on heat transfer. Their studies showed that various ridge shapes have comparable thermal performance and the composite-ribbed performed best in their ribbed configurations. Liou et al. [14] also studied the effect of divider thickness on the local heat transfer distributions. Their results showed that the direction and strength of the secondary flow are the most important fluid dynamic factors affecting the heat transfer distributions, followed by the convective mean velocity and then the turbulent kinetic energy.

The previous studies focused on the investigations of turbulator effects on heat transfer in uniform flows, and indicated that the turbulators have substantial effects on heat transfer rates. Fans have been widely used in electronics and computers to induce fluid motions for heat transfer applications. The fan itself is a good turbulator, which generates vortical flow motions. The studies of an external turbulator effect on heat transfer and flow characteristics in such inherently vortical fan flows have not been seen in literatures, which motivates this research. Cross-sectional flow velocities were first measured to characterize the flow structures. Three near-wall flow parameters, including the axial mean velocity, axial vorticity and turbulent kinetic energy, were then obtained from three-component mean and fluctuating velocities. Temperature distributions on a heated aluminum plate, acting as the heat transfer surface, were measured to obtain the Nusselt numbers. The turbulator effects on the flow and heat transfer characteristics were discussed.

2. Experimental setup and methods

2.1. Experimental setup

The primary experimental setup utilized in this research is shown in Fig. 1. An open-circuit wind tunnel system was used to develop uniform flows with turbulence intensities less than 1 percent inside a 7 x 7 cm^2 duct. Air was supplied to the 50 *cm* long test section by a blower, and passed through a turbulence-management section that includes a diffuser, honeycombs, screens and a contraction section. An axial *DC* fan was placed between the contraction section and the test section to develop fan flows inside the duct, where the diffuser, honeycombs and screens were removed from the wind tunnel system. The 8 x 8 cm^2 fan has seven blades with the maximum airflow of 45.2 *CFM*, produced by Yen-Sun Tech, Taiwan. A delta-wing with 40^o angle of attack was used as a turbulator, which is placed on the bottom wall of the duct, 10 *cm* downstream of the turbulence-management section or the fan, see Figs. 1 and 2. The base width and tip height of the delta-wing are 7 and 3.5 *cm*, respectively. The origin of the coordinate system used for data presentation is at the delta-wing location. An aluminum plate, 4 x 20 cm^2, was

fixed to the bottom wall of the test section, 20 *cm* downstream of the delta-wing between *X/D*=2.856 and 5.712 to serve as the heat transfer surface. The 4 *cm* width of this aluminum plate is smaller than the duct width to reduce the corner-effect on heat transfer, where secondary vortices or corner vortices possibly occur at duct corners. The investigated flows include the fan flows and uniform flows with and without the delta-wing vortex generator.

2.2. Velocity measurement

Three-component, mean and fluctuating velocity measurements were performed using a TSI laser Doppler velocimetry (LDV). A new test section, made of plexiglass to provide optical access, was used for the velocity measurements. The duct average velocities were 1 *m/s*, 1.62 *m/s*, 2.13 *m/s* and 2.67 *m/s*, where the corresponding Reynolds numbers are 4430, 7200, 9440 and 11820, respectively, based on the duct hydraulic diameter. These measurements were conducted at 121 locations in each *Y-Z* plane, see Fig. 3, at four *X/D* stations of 1.428, 2.856, 4.284 and 5.712, and 140 locations in each *X-Y* plane at two *Z/D* stations of -0.286 and 0.286 to characterize the flow structures. Each velocity was calculated from 4096 collected velocity samples. The mean velocity ($\overline{\mathrm{V}}$) is the averaged value of the 4096 velocity samples and the fluctuating velocity is obtained from $\sqrt{(\sum \mathrm{v}^2)/4096 - \overline{\mathrm{v}}^2}$, where v is the local instant velocity. The cross-sectional axial component of vorticity (axial vorticity) at each *Y-Z* plane was obtained from the 242 *Y*- and *Z*-component mean velocities. The circulation of a small block, see Fig. 3, was first calculated using the velocities at the block corners. The cross-sectional axial vorticity was the 100-block circulations divided by the 100-block area. Three-component velocity measurements near the heat transfer surface were also conducted because these velocities play an important role in heat transfer characteristics. These near-wall velocity measurements were conducted at 72 locations between *Y*=0.2 and 1.6 *cm* (*Y/D*=0.0286 and 0.2286), see Fig. 3, at two *X/D* stations of 2.856 and 5.712, which cover the uniform-flow velocity boundary layers conducted in this research. The near-wall axial vorticity was obtained from the mean *Y*- and Z-components velocities, calculated similar to that of the cross-sectional axial vorticity. The particles for the LDV measurements were generated by a smoke wire located upstream of the apparatus. Particle diameters in the sub-micron range have been shown to be able to follow turbulence frequencies exceeding 1 KHz [15]. The uncertainty in the velocity measurements was estimated to be less than 5 percent.

2.3. Heat transfer measurement

The heat transfer coefficient, $h=\dfrac{Q_{in}-Q_{loss}}{A(T_w-T_0)}$, was measured on the heat transfer surface (aluminum plate). The heat transfer plate consists of the 4 x 20 cm^2, 1 *mm* thick, aluminum plate (heat transfer surface), a heating plate, two electrical insulation plates and a fiberglass plate, see Fig. 2. Electrical power was continuously supplied to the heating plate from a *DC* power supply, resulting in a constant-heat-flux heat transfer surface. The air inlet temperature, T_0, is the reference temperature, obtained by a type-T, 0.1 *mm*-diameter thermocouple placed at the contraction section of the wind tunnel. The temperatures were read using a TempScan/1100 system produced by IOtech, Inc, with the uncertainty within 0.5^oC. The surface temperatures, T_w, of the heated aluminum plate were measured using 25 thermocouples. The junction beads of thermocouples were cemented, using thermally conducting epoxy, in small holes on the back of the aluminum plate approximately 0.5 *mm* from the top surface. The obtained temperatures were negligibly different from the surface temperatures due to the thin and highly

conductive aluminum plate. The averaged temperature from the 25 thermocouples is used to calculate the average heat transfer coefficient on the heat transfer surface. The power input, Q_{in}, to the heating plate is 12.4 watt with 3 percent uncertainty, resulting in the surface temperatures between 50^oC and 85^oC with the uncertainty of 1^oC from repeatability tests. Eight more thermocouples were placed in the insulation fiberglass plate, six on the heating side and two on the ambient side of the plate. The averaged temperatures from the six and two thermocouples, respectively, are used to determine the temperature drop through the plate. Heat conduction loss through the back of the heating plate is calculated using the Fourier's law, which is estimated to be less than 3 percent of the total heat generated. Radiation loss is estimated to be less than 3.6 percent of the total heat flux. Conduction loss along the sides of the heat transfer plate accounted for a small fraction and was neglected. The total uncertainty in the measurement of the heat transfer coefficient was estimated to be within 10 percent.

3. Results and Discussion

3.1. Cross-sectional flow characteristics

The cross-sectional flow structures in the *Y-Z* and *X-Y* planes for the investigated flows were first discussed. Figures 4(a-c) present typical secondary flow velocity vectors in *Y-Z* planes looking in downstream flow direction. The uniform flow across the delta-wing generates two vortices of different directions, and the fan generates a symmetrical, counterclockwise vortical flow. Also, the secondary flow velocities for the fan flow are much larger than those for the uniform flow across the delta-wing, see Figs. 4(a) and 4(b). It is noted from Fig. 4(c) that the secondary flow structure for the fan flow across the delta-wing is generally similar to that for the fan flow though the vortex center was slightly lifted upward. This is possibly due to the flow blockage by the bottom-wall delta-wing that diverts the flow a little upward. The secondary flow structures for the investigated flows at different *X/D* stations are qualitatively similar to those shown in Figs. 4(a-c), respectively, but with small velocities as the vortices develop downstream.

Figures 5(a-f) present typically mean flow velocity vectors in *X-Y* planes. Note that the delta-wing has 40^o angle of attack. Its base is at *X/D*=0, and its tip point is at *Y/D*=0.5 and *Z/D*=0. Figures 5(a-b) show that a close recirculation zone occurred in the immediate neighborhood behind the delta-wing at *Z/D*=-0.286, while no reversed flow was observed at *Z/D*=0, for the uniform flow across the delta-wing. As the flow develops downstream, the delta-wing effect on the flow structures become less. The flows were vortical at the inlets of the heat transfer surface (*X/D*=2.856) with the flow velocities slightly smaller and larger than the duct averaged velocity (2.13 *m/s*) at *Z/D*=-0.286 and 0, respectively, and with the velocity components slightly toward the heat transfer surface. Figures 5(c-d) show that the fan flow has downward and upward velocity components at *Z/D*=-0.286 and 0.286, respectively, due to counterclockwise rotation of the vortical flow motion. The delta-wing effects on the fan-flow structures are presented in Figs. 5(e-f). A very small reversed flow region was observed at *Z/D*=0.286, while no reversed flows occurred at *Z/D*=-0.286. It is noted that the fan flow is counterclockwise rotated as it develops downstream. On the up-wash side of the vortex (*Z/D*=0.286), the flows are blocked by the delta-wing that causes the decrease in flow velocities downstream of the delta-wing. The flows are accelerated at Z/D=-0.286 to maintain the constant flow rate at each cross section of the confined duct flow. The delta-wing effect on the fan-flow structures becomes less as the vortex develops downstream. Figures 5(c-f) show that the flow characteristics at the inlets of the heat transfer surface are generally similar between the fan flows with and

without the delta-wing. It can be expected that the complicated flow structures in the immediate neighborhood behind the delta-wing should have different effects on heat transfer, which will be discussed in other paper.

The cross-sectional normalized axial vorticity, $(\eta D/U_d)_{CS}$, distributions for the investigated flows of Re_D=11820 are shown in Fig. 6, where the axial vorticity of the uniform flow across the delta-wing is the magnitude sum of the two opposite vortices. Figure 6 shows that the fan generates stronger vortices than the uniform flow across the delta-wing, and the vortex strengths decrease as the vortices develop downstream. The values of $(\eta D/U_d)_{CS}$ are 4.76 and 3.19 at X/D=1.428 and 5.712, respectively, for the fan flow, and are 2.31 and 0.77 at X/D=1.428 and 5.712, respectively, for the uniform flow across the delta-wing. The loss in the axial vorticity for the fan flow (33 percent) is less than that for the uniform flow across the delta-wing (67 percent) from X/D=1.428 to 5.712. The vortex generated by the fan persists further downstream than that generated by the uniform flow across the delta-wing. Figure 6 also shows that the delta-wing in fan flows has little effect on the axial vorticity, which causes a little increase and decrease at X/D=1.428 and 5.712, respectively. This result should be due that the fan-generated vortex is strong enough such that the vortex structure is only slightly disturbed by the delta-wing, as discussed in Figs. 4(b-c). It is also possibly caused by the interaction of vortex systems generated by the fan and the delta-wing. It is noted from Fig. 4(a) that the uniform flow across the delta-wing produced a counter-rotating vortex system, where the two vortices have different direction of rotation. The interactions of these two vortices may result in additive and subtractive effects in vortex strength and, thus, the net effect becomes insignificant.

3.2. Flow characteristics near the heat transfer surface

The axial mean velocities, the axial vorticities and the turbulent kinetic energy near the heat transfer surface were investigated next because the near-wall flow characteristics should have major effects on heat transfer. Measurements showed that the boundary-layer thicknesses for the uniform flows of the investigated Reynolds numbers over the heat transfer surface were between 9 and 13 *mm*. Typical measured boundary-layer velocity profiles at X/D=2.856, Z/D=0 are shown in Fig. 7. The exact Blasius solution for a laminar flow over a flat plate is also presented for comparison, which shows good agreements between the theory and experiments. The velocity data between Y=2 and 12 *mm* for the flows of Re_D=9440 and 11820, and between Y=2 and 14 *mm* for the flows of Re_D=4430 and 7200 were, thus, used to calculate the near-wall flow parameters.

3.2.1. Axial mean velocity (convective effect)

The axial mean velocity is an indication of the convective effect on heat transfer. Its magnitude is expected to be proportional to the convective heat transfer rate. Figures 8(a-c) present some results of the near-wall axial mean velocity contours for the investigated flows of Re_D=11820 at X/D=2.856, showing the profound effects of vortices on the velocity distributions. The near-wall axial mean velocity distributions are completely different from the uniform-flow boundary-layer velocity distribution. Figure 8(a) shows that the velocities on the left and right sides of the flow region are smaller than those on the central region for the uniform flow across the delta-wing. Figures 8(b-c) indicate that the velocities on the left sides of the flow region are larger than those on the right sides of the flow region for both the fan flows with and without the delta-wing, due to the vortex characteristics as presented in Figs. 4(a-c). On the up-wash side of the vortex, low-speed fluid is lifted away from the wall, while on the downwash side of the vortex, high-speed fluid is swept into the near wall region. These findings are consistent with the results by Eibeck et al [3]. These figures also show that the near-wall axial mean velocities are mostly

larger than the duct average velocity.

The averaged axial mean velocity, U_{av}, averaged form the near-wall axial mean velocities, is used to represent the overall convective effect on heat transfer. Figure 9 presents the variations of the normalized averaged axial mean velocity, U_{av}/U_d, with Reynolds number for the investigated flows at X/D=2.856 and 5.712, showing the weak dependence of U_{av}/U_d on Reynolds number. The averaged axial mean velocities slightly decrease from X/D=2.856 to X/D=5.712 for the fan flows, while there is up to 22 percent decrease for both fan and uniform flows across the delta-wing. Because of the constant flow rate in each duct cross section, this result reveals that the delta-wing causes the near-wall flow deceleration as the flows develop downstream.

3.2.2. Axial vorticity (secondary-flow effect)

Large strength of the secondary flow is expected to have a large effect on heat transfer. Figure 10 presents the variations of the near-wall normalized axial vorticity, $(\eta D/U_d)_{NW}$, with Reynolds number for the investigated flows at two X/D stations of 2.856 and 5.712. The normalized axial vorticities generally remain constant with Reynolds numbers, and decrease as the flows develop downstream. Larger axial vorticities are generated in fan flows than in uniform flows across the delta-wing, as expected. It has been shown in Fig. 9 that the delta-wing in the investigated flows causes the near-wall flow deceleration from X/D=2.856 to 5.712, which possibly results in the near-wall flow relaminarization. As a result, the fan flows across the delta-wing have larger and smaller axial vorticity than the fan flows at X/D=2.856 and X/D=5.712, respectively. The delta-wing vortex generator has, thus, little overall effect on the near-wall axial vorticity over the heat transfer surface.

3.2.3. Turbulent kinetic energy (turbulence effect)

The turbulent kinetic energy, $k^2=(\overline{U'^2}+\overline{V'^2}+\overline{W'^2})/2$, was obtained from the X-, Y- and Z-component fluctuating velocities. Large turbulent kinetic energy is expected to have a large effect on heat transfer rate. Figure 11 presents the variations of the near-wall normalized turbulent kinetic energy, k^2/U_d^2, with Reynolds number for the investigated flows at X/D=2.856 and 5.712, showing the weak dependence of k^2/U_d^2 on Reynolds number. The delta-wing increases the turbulent kinetic energy up to 80 percent both in fan flows and uniform flows. However, it causes the turbulent kinetic energy decrease fast as the vortices develop downstream. Figure 11 indicates that the turbulent kinetic energy at X/D=5.712 for the fan flows across the delta-wing is approximately 10 percent less than that for the fan flows. The fast decrease in the turbulent kinetic energy caused by the delta-wing is also possibly due to the near-wall flow relaminarization as discussed above. The overall effect of the delta-wing vortex generator is to increase the turbulent kinetic energy over the heat transfer surface in fan flows and uniform flows.

3.3. Heat transfer characteristics

The heat transfer characteristics on the heat transfer surface are presented in a dimensionless form as the Nusselt number, $Nu=hD/k$. The Nusselt numbers on the heat transfer surface for the uniform flows of the investigated Reynolds numbers were also measured and compared with the analytical unheated starting length solutions presented in Kays and Crawford [16] to check the accuracy of the measured heat transfer data. Figure 12 shows that the Nusselt number distribution is approximately 6 percent higher than the predictions, which is under the uncertainty estimate. Due to the vortical flow motions, the fan flows and the uniform flows across the delta-wing have much better heat transfer performance than the uniform flows. Also, the Nusselt numbers increase as the Reynolds numbers increase, and the Nusselt numbers are higher for the fan flows than the uniform flows

across the delta-wing. The delta-wing in uniform flows causes large increase in the Nusselt number, while it has little effect on heat transfer rates in fan flows in the investigated *X/D* ranges.

3.4. Relations between heat transfer and flow characteristics

It has been shown above that larger near-wall averaged axial mean velocity, axial vorticity and turbulent kinetic energy occurred in fan flows and uniform flows across the delta-wing than in uniform flows. As a result, the vortical flows have higher heat transfer rates than the uniform flows. Figure 13 presents the Nusselt number ratios between the investigated flows and the uniform flows, Nu_x/Nu_0, and between the fan flows with and without the delta-wing, Nu_3/Nu_2. The increases in Nusselt numbers for the fan flows and uniform flows across the delta-wing were up to 115 percent and 65 percent, respectively. The delta-wing has large effect on heat transfer augmentation in uniform flows. However, the delta-wing in inherently vortical fan flows has little effect on heat transfer in the investigated *X/D* ranges. The values of Nu_3/Nu_2 are approximately 1.02 for all of the investigated Reynolds numbers. To elucidate the relations between the near-wall flow parameters and the heat transfer in fan flows, two 4 x 5 cm^2 heat transfer plates were placed between *XD*=2.5 and 3.214, and between *XD*=5.357 and 6.071, respectively, for heat transfer measurements. Nine thermocouples were embedded on each heat transfer plate, and the averaged temperature from these 9 thermocouples was used to calculate the Nusselt number on that plate. Figure 13 shows that the Nusselt number ratios between the fan flows with and without the delta-wing for the heat transfer plate placed between *X/D*=2.5 and 3.214, $(Nu_3/Nu_2)_{X/D=2.856}$, are approximately 1.05 for all of the investigated Reynolds numbers. Figures 9-11 have shown that the near-wall averaged axial mean velocities and axial vorticities in fan flows were a little increased, while the turbulent kinetic energy was largely increased, by the delta-wing at *X/D*=2.856. If the turbulent kinetic energy induced by the delta-wing plays an important role in heat transfer, the Nusselt number for the fan flows with the delta-wing should, accordingly, be largely increased. These results suggest that the turbulent kinetic energy in fan flows should not have a dominated effect on heat transfer rate. The near-wall averaged axial mean velocities, axial vorticities and turbulent kinetic energy for the fan flows across the delta-wing were slightly smaller than those for the fan flows without the delta-wing at *X/D*=5.712. Thus, the delta-wing has little effect on heat transfer rate at *X/D*=5.712, where the Nusselt number ratios for the heat transfer plate placed between *X/D*=5.357 and 6.071, $(Nu_3/Nu_2)_{X/D=5.712}$, are approximately 0.97.

3.5. Practical significance

Fans have been widely used in electronics and computers as the pumping sources to induce flow motions for heat transfer applications. The fan generates vortical flow motions that result in higher heat transfer rates than the uniform flows. The needs for even faster heat transfer rates are urgent, for example, in CPU cooling of modern computers. An understanding of the fan-flow characteristics and their relations with the heat transfer would be helpful to improve the heat transfer rate for engineering applications. The delta-wing vortex generator in uniform flows augments the heat transfer. However, it has negligible effect on heat transfer augmentation in fan flows in the investigated *X/D* ranges. One of the possible reasons is due to the cancellation of the vortex systems generated by the fan and the delta-wing vortex generator. Other types of vortex generator may have different effect on heat transfer. The other possible reason is that the delta-wing effect on the near-wall flow characteristics does not persist downstream enough. This research has shown that the fan-flow structures were largely disturbed in the immediate neighborhood behind the vortex generator, which should have large effects on heat transfer. These results provide

some hopes and methods to possibly augment heat transfer in fan flows, and are recommended for further studies.

4. Conclusions

Effects of an external delta-wing vortex generator on the flow and heat transfer characteristics in fan flows and uniform flows were experimentally investigated and compared. Several conclusions were drawn from the results of this research:

(1) The delta-wing vortex generator in fan flows has little overall effect on the near-wall averaged axial mean velocity and axial vorticity, but increases the turbulent kinetic energy, in the investigated *X/D* ranges.

(2) The delta-wing vortex generator in fan flows causes the near-wall averaged axial mean velocity, axial vorticity and turbulent kinetic energy decrease fast as the flows develop downstream due to the near-wall flow relaminarization.

(3) The near-wall axial vorticity and turbulent kinetic energy are much larger in fan flows than in uniform flows with the delta-wing. As a result, higher heat transfer rate occurs in fan flows than in uniform flows with the delta-wing.

(4) The delta-wing vortex generator largely augments the heat transfer in uniform flows, while it has little effect on heat transfer augmentation in fan flows, in the investigated *X/D* ranges. The turbulent kinetic energy induced by the delta-wing vortex generator in fan flows should not have an important effect on heat transfer augmentation.

(5) The fan-flow structures are largely disturbed in the immediate neighborhood behind the delta-wing vortex generator, where the heat transfer would possibly be augmented. Other types of vortex generator may have different heat transfer effect than the delta-wing vortex generator. Further studies are, thus, recommended.

Nomenclature

A	surface area of the heated plate (0.008 m^2)
D	duct hydraulic diameter (0.07 m)
h	heat transfer coefficient (W/m^2K)
k	thermal conductivity of the air, evaluated at film temperature (W/mK)
k^2	near-wall turbulent kinetic energy (m^2/s^2)
Nu	Nusselt number
Q_{in}	power input to the heated plate (W)
Q_{loss}	conduction and radiation losses (W)
Re_D	Reynolds number based on the duct hydraulic diameter
T_w	surface temperature of the heated plate (K)
T_o	inlet air temperature (K)

U_{av}	near-wall averaged axial mean velocity (*m/s*)
U_c	duct center velocity (*m/s*)
U_d	duct average velocity (*m/s*)
U'	*X*-component fluctuating velocity (*m/s*)
U	near-wall axial mean velocity (*m/s*)
V'	*Y*-component fluctuating velocity (*m/s*)
v	local instant velocity (*m/s*)
$\overline{\mathrm{v}}$	local mean velocity (*m/s*)
W'	Z-component fluctuating velocity (*m/s*)
X	spatial coordinate, axial direction
Y	spatial coordinate, normal direction
Z	spatial coordinate, spanwise direction
η	axial vorticity (*1/s*)
ν	kinematic viscosity of the air (m^2/s)

Acknowledgement

This research was sponsored by the National Science Council of the Republic of China under contract NSC91-2212-E032-007.

References

1. F. J. Edwards, C. J. R. Alker, The improvement of forced convection surface heat transfer using surface protrusions in the form of cubes and vortex generators, Proceedings of the Fifth International Heat Transfer Conference, Tokyo, 1974, Vol. 2, pp. 244-248.
2. C. M. B. Russell, T. V. Jones, G. H. Lee, Heat transfer enhancement using vortex generators, Proceedings of the Seventh International Heat Transfer Conference, Munich, 1982, Vol. 3, pp. 283-288.
3. P. A. Eibeck, J. K. Eaton, Heat transfer effects of a longitudinal vortex embedded in a turbulent boundary layer, Journal of Heat Transfer, 109 (1987) 16-24.
4. A. Y. Turk, G. H. Junkhan, Heat transfer enhancement downstream of vortex generators on a flat plate, Proceedings of the Eighth International Heat Transfer Conference, San Francisco, CA, 1986, pp. 2903-2908.
5. M. Fiebig, P. Kallweit, N. Mitra, S. Tiggelbeck, Heat transfer enhancement and drag by longitudinal vortex generators in channel flow, Experimental Thermal and Fluid Science, 4 (1991) 103-114.
6. S. Tiggelbeck, N. Mitra, M. Fiebig, Flow structure and heat transfer in a channel with multiple longitudinal vortex generators, Experimental Thermal and Fluid Science, 5 (1992) 425-436.
7. S. Tiggelbeck, N. Mitra, M. Fiebig, Experimental investigations of heat transfer enhancement and flow losses in

a channel with double rows of longitudinal vortex generators, International Journal of Heat and Mass Transfer, 36 (9) (1993) 2327-2337.

8. S. Tiggelbeck, N. Mitra, M. Fiebig, Comparison of wing-type vortex generators for heat transfer enhancement in channel flows, Journal of Heat Transfer, 116 (1994) 880-885.
9. G. Biswas, P. Deb, S. Biswas, Generation of longitudinal streamwise vortices – a device for improving heat exchanger design, Journal of Heat Transfer, 116 (1994) 588-597.
10. G. Biswas, K. Torii, D. Fujii, K. Nishino, Numerical and experimental determination of flow structure and heat transfer effects of longitudinal vortices in a channel flow, International Journal of Heat and Mass Transfer, 39 (16) (1996) 3441-3451.
11. S. V. Ekkad, J. C. Han, Detailed heat transfer distributions in two-pass square channels with rib turbulators, International Journal of Heat and Mass Transfer, 40 (11) (1997).
12. J. P. Tsia, J. J. Hwang, Measurements of heat transfer and fluid flow in a rectangular duct with alternate attached-detached rib-arrays, International Journal of Heat and Mass Transfer, 42 (1999) 2071-2083.
13. T. M. Liou, J. J. Hwang, Effect of ridge shapes on turbulent heat transfer and friction in a rectangular channel, International Journal of Heat and Mass Transfer, 36 (4) (1993) 931-940.
14. T. M. Liou, C. C. Chen; Y. Y. Tzeng, T. W. Tsai, Non-intrusive measurements of near-wall fluid flow and surface heat transfer in a serpentine passage, International Journal of Heat Mass Transfer 43 (2000) 3233-3244.
15. F. Durst, A. Melling, J. H. Whitelaw, Principles and Practice of Laser Doppler Velocimetry. Academic Press, New York, 1976 (Chapter 9).
16. W. M. Kays, M. E. Crawford, Convective Heat and Mass Transfer, 2nd ed., New York: McGraw-Hill, 1980.

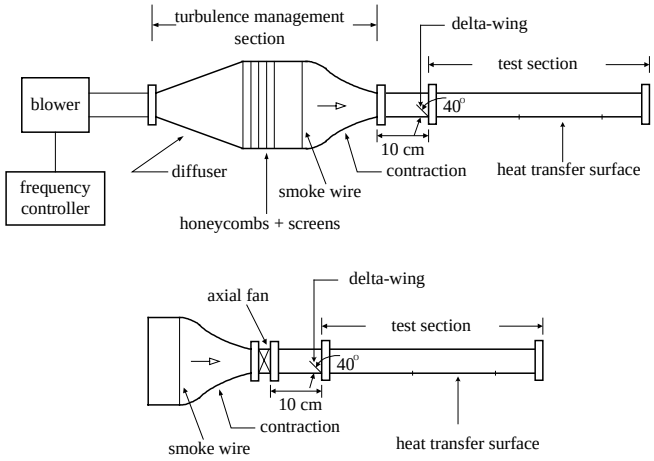

Figure 1: The experimental setup for the uniform flow and fan-flow system.

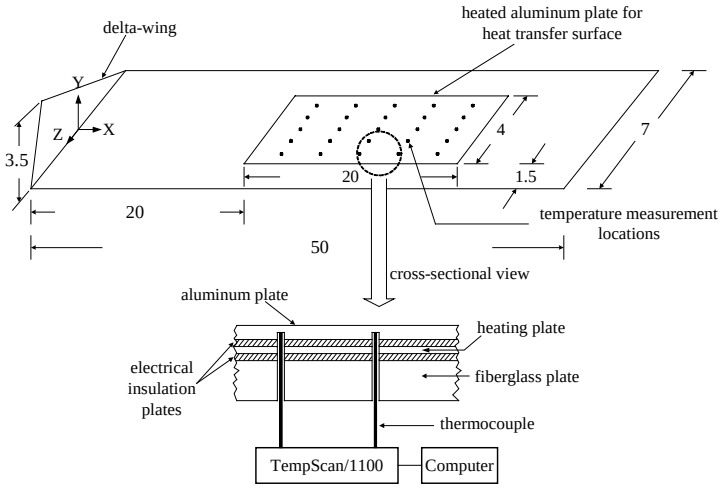

Figure 2: The bottom wall of the test section, showing the delta-wing, the coordinate system, the heat transfer surface and the temperature measurement locations (unit: cm).

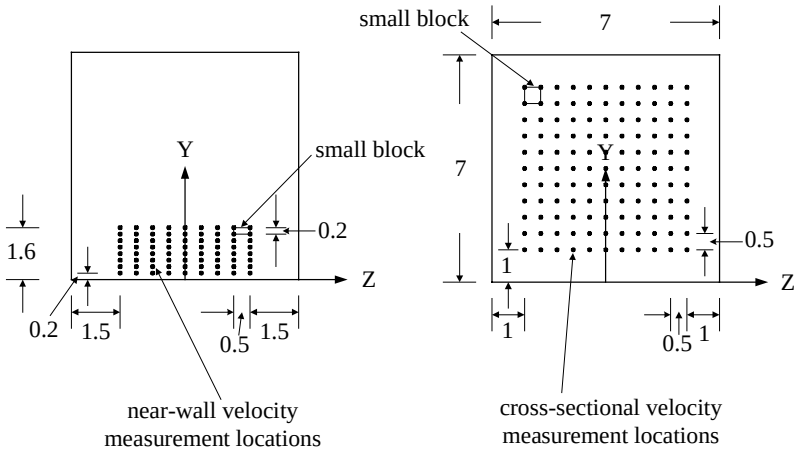

Figure 3: The cross-sectional view of the duct, showing the velocity measurement locations and the small blocks for the calculation of axial vorticities(unit: cm).

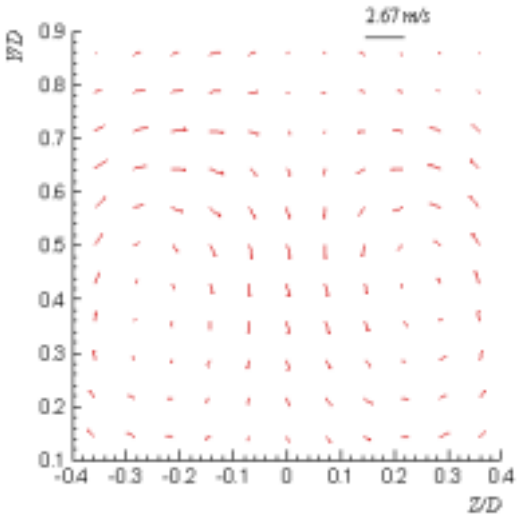

Figure 4(a): The secondary flow velocity vectors for the uniform flow of Re_D=11820 with delta-wing at X/D=2.856.

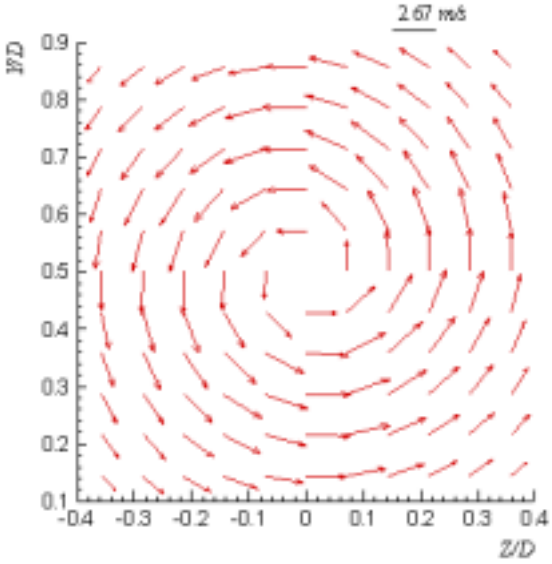

Figure 4(b): The secondary flow velocity vectors for the fan flow of Re_D=11820 at X/D=2.856.

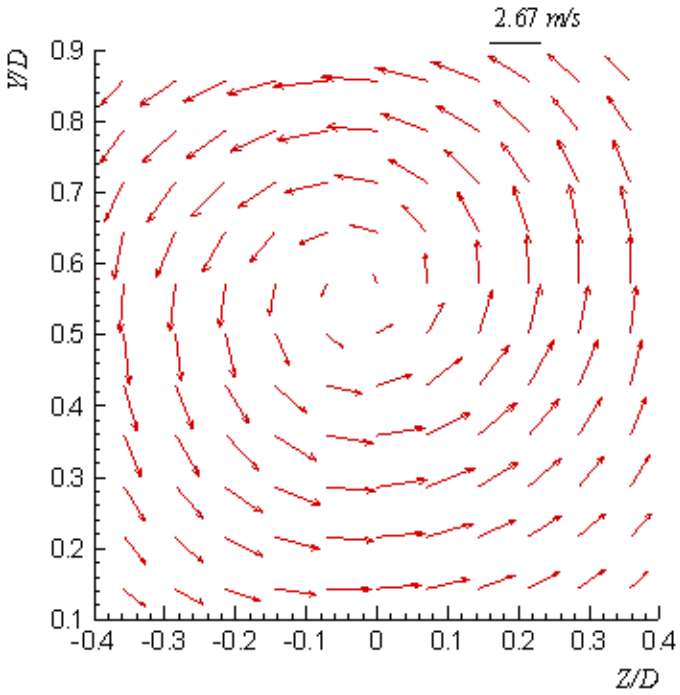

Figure 4(c): The secondary flow velocity vectors for the fan flow of Re_D=11820 with delta-wing at X/D=2.856.

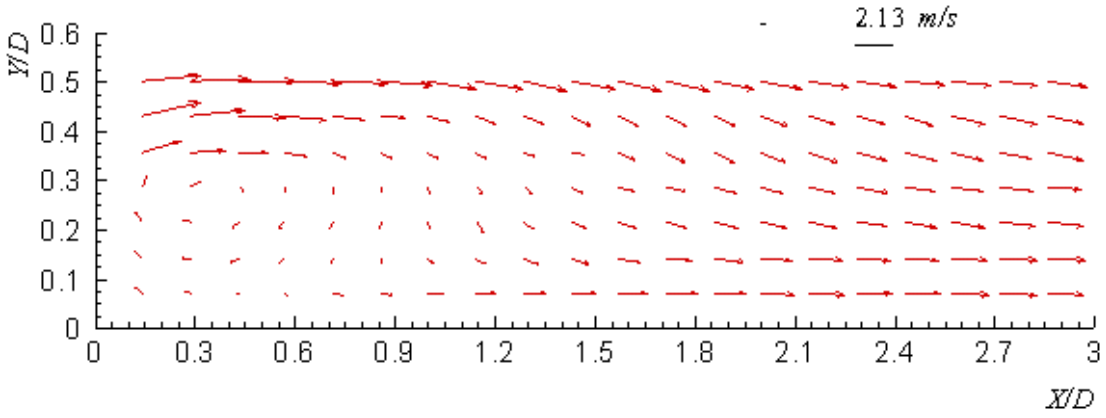

Figure 5(a) : The mean flow velocity vectors in the *X-Y* plane for the uniform flow of Re_D=9440 with delta-wing at *Z/D*=-0.286.

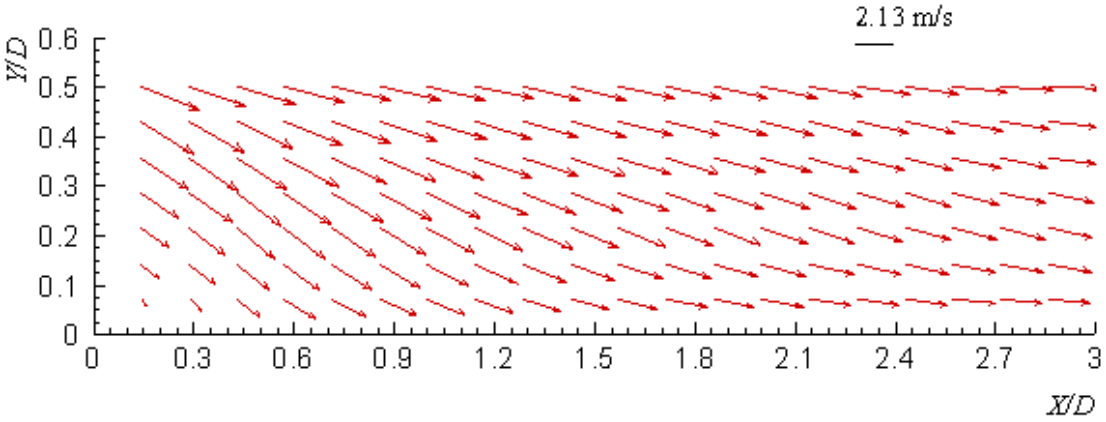

Figure 5(b) : The mean flow velocity vectors in the *X-Y* plane for the uniform flow of Re_D=9440 with delta-wing at *Z/D*=0.

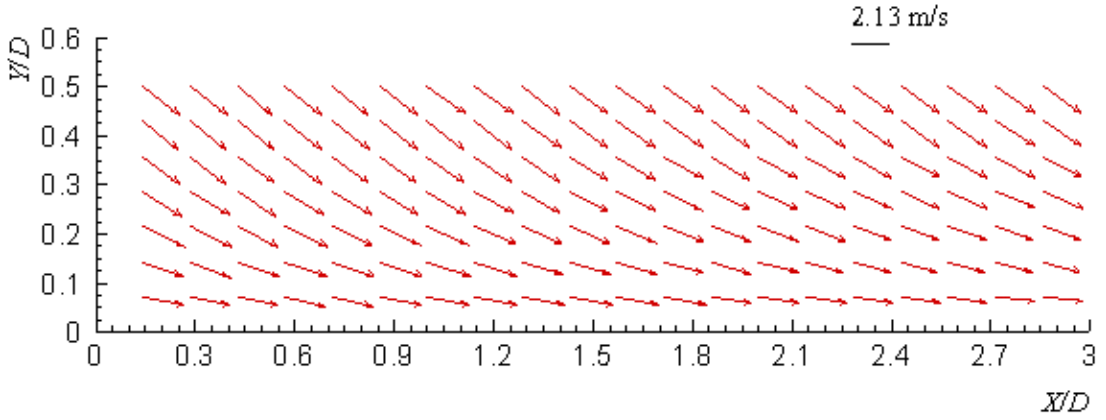

Figure 5(c) : The mean flow velocity vectors in the *X-Y* plane for the fan flow of Re_D=9440 at *Z/D* =-0.286.

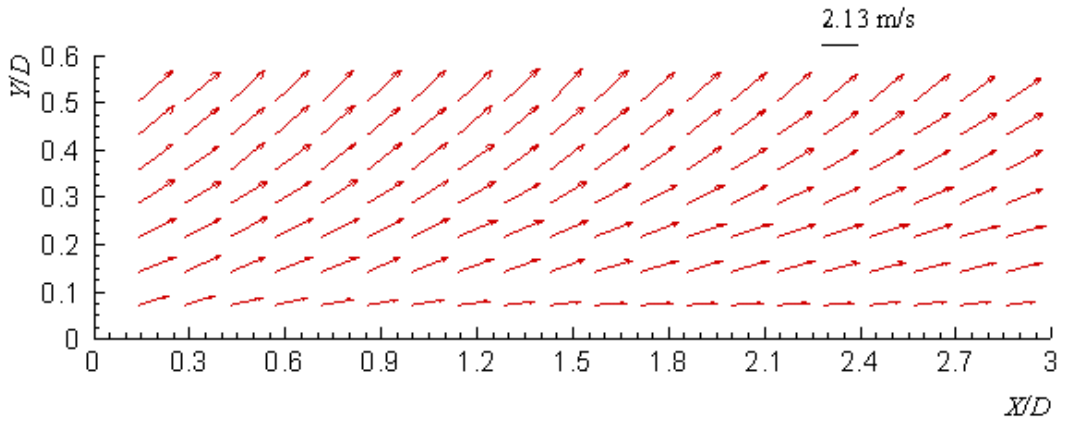

Figure 5(d) : The mean flow velocity vectors in the *X-Y* plane for the fan flow of Re_D=9440 at *Z/D*=0.286.

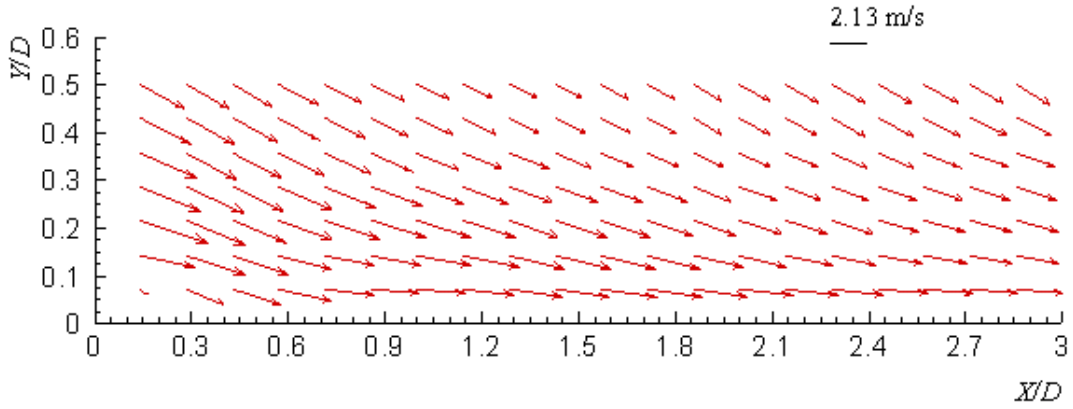

Figure 5(e) : The mean flow velocity vectors in the *X-Y* plane for the fan flow of Re_D=9440 with delta-wing at *Z/D*=-0.286.

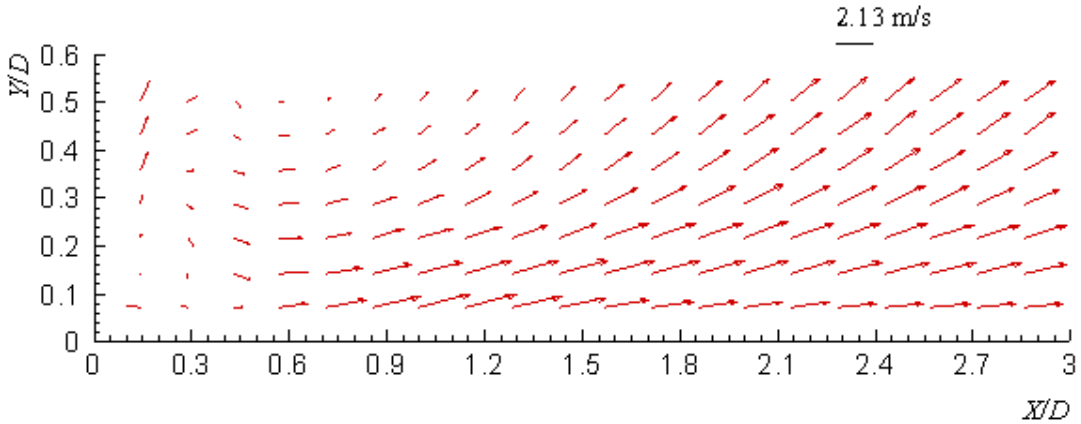

Figure 5(f) : The mean flow velocity vectors in the *X-Y* plane for the fan flow of Re_D=9440 with delta-wing at *Z/D*=0.286.

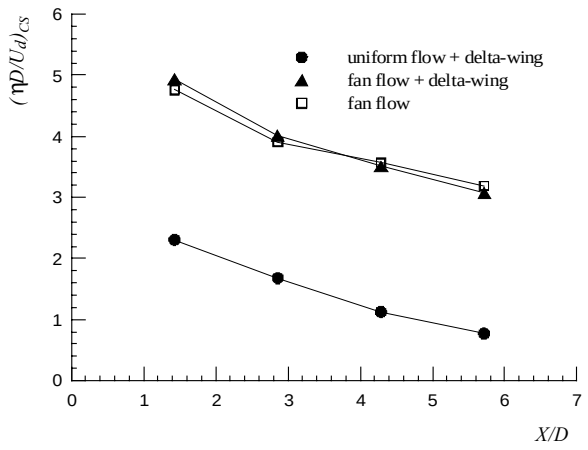

Figure 6: The cross-sectional normalized vorticity, $(\eta D/U_d)_{CS}$, distributions for the three investigated flows of Re_D=11820 (U_d =2.67m/s).

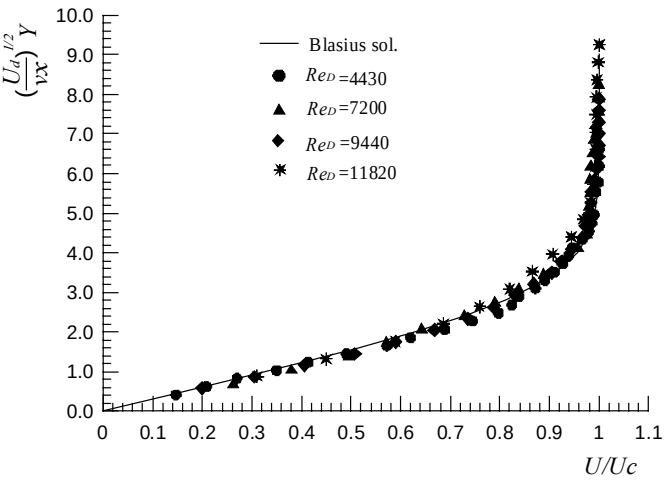

Figure 7: The measured boundary-layer velocity profiles for the uniform flows of investigated Reynolds numbers and the theoretical Blasius solution.

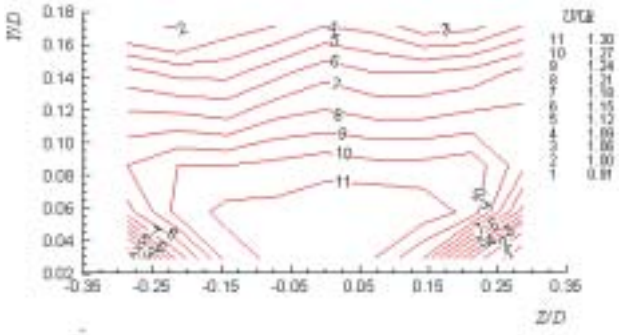

Figure 8(a): The near-wall axial mean velocity contours for the uniform flow of Re_D=11820 with delta-wing at X/D=2.856.

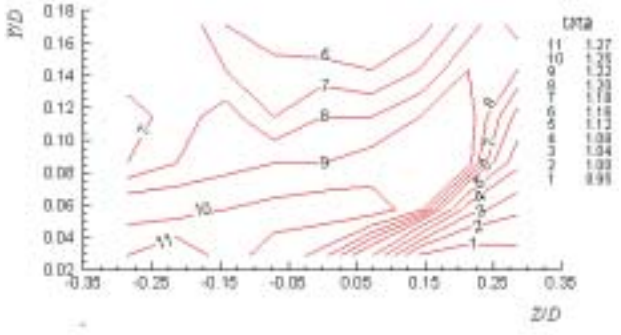

Figure 8(b): The near-wall axial mean velocity contours for the fan flow of Re_D=11820 at X/D=2.856.

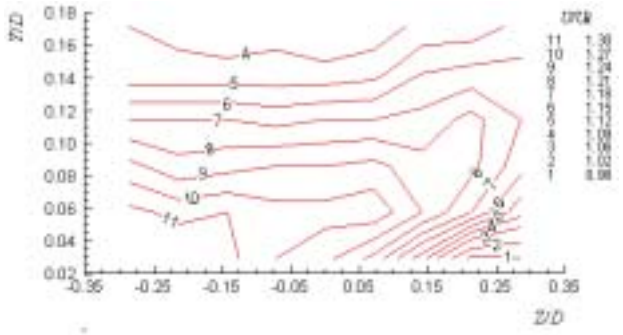

Figure 8(c): The near-wall axial mean velocity contours for the fan flow of Re_D=11820 with delta-wing at X/D=2.856.

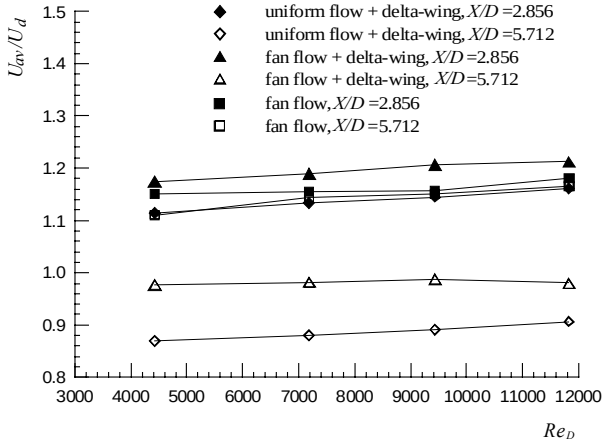

Figure 9: The near-wall averaged axial mean velocities, U_{av}/U_d, of the investigated flows at X/D=2.856 and 5.712 vs. Reynolds number.

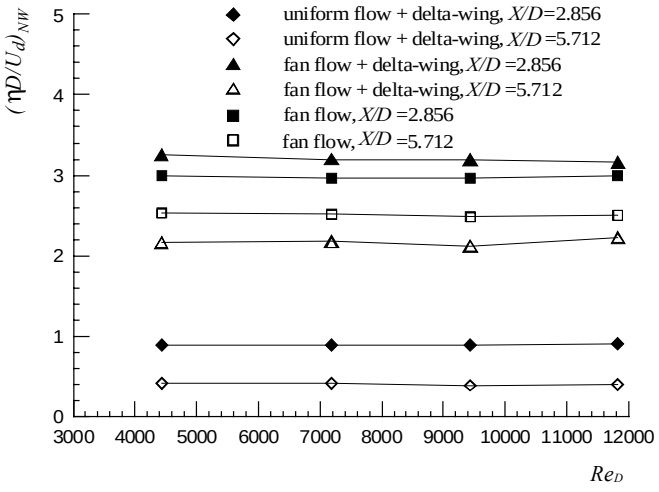

Figure 10: The near-wall normalized axial vorticities, $(\eta D/U_d)_{NW}$, of the investigated flows at X/D =2.856 and 5.712 vs. Reynolds number.

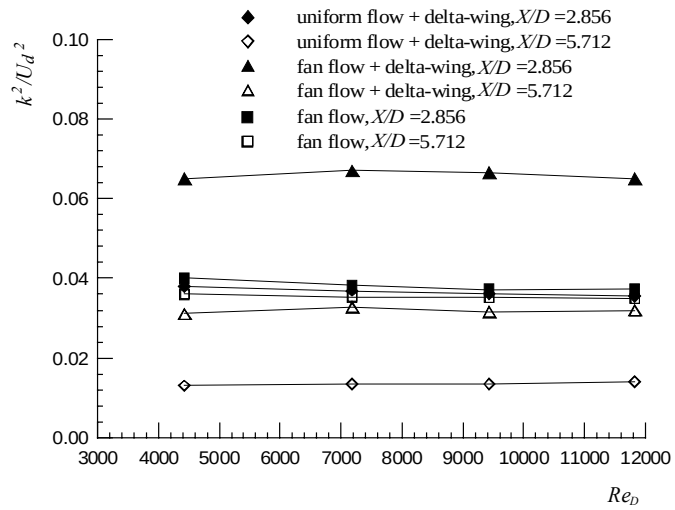

Figure 11: The near-wall normalized turbulent kinetic energy, k^2/U_d^2, of the investigated flows at X/D =2.586 and 5.712 vs. Reynolds number.

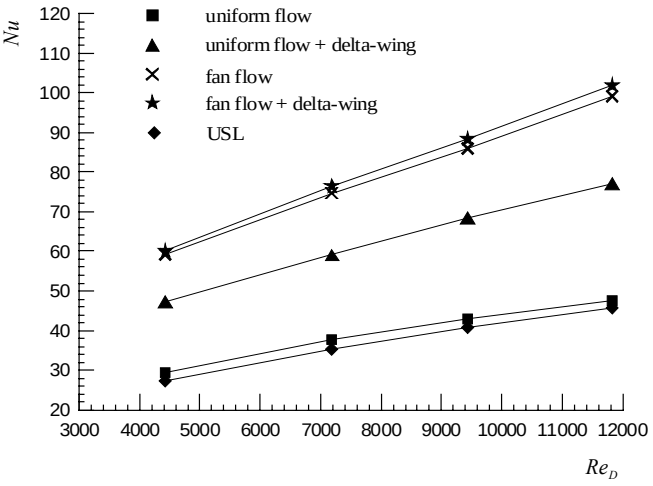

Figure 12: The Nusselt numbers, Nu, on the heat transfer surface of the inverstgated flows vs. Reynolds number and the analytical unheated starting length solutions (USL).

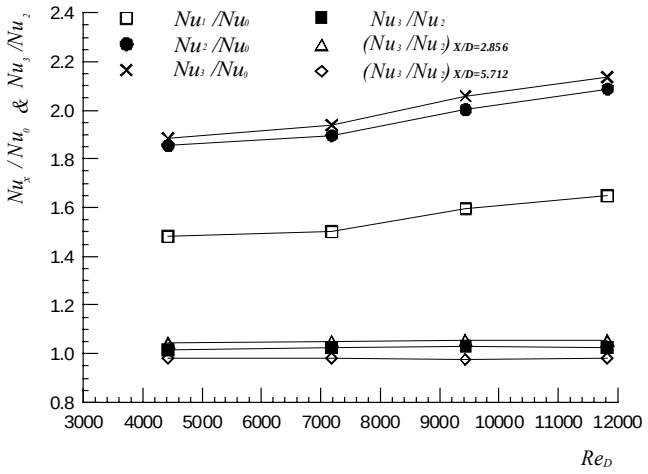

Figure 13: The Nusselt number ratios between the investigated flows and uniform flows, Nu_x/Nu_0, and between the fan flows with and without delta-wing, Nu_3/Nu_2, where Nu_0, Nu_1, Nu_2, Nu are the Nusselt numbers of the uniform flows without and with delta-wing, the fan flows without and with delta-wing, respectively.